

HiGRAPH: A Large-Scale Hierarchical Graph Dataset for Malware Analysis

Han Chen
University of Technology Sydney
Sydney, Australia
han.chen-7@student.uts.edu.au

Hanchen Wang
University of Technology Sydney
Sydney, Australia
hanchen.wang@uts.edu.au

Hongmei Chen
Yunnan University
Kunming, China
hmchen@ynu.edu.cn

Ying Zhang
University of Technology Sydney
Sydney, Australia
ying.zhang@uts.edu.au

Lu Qin
University of Technology Sydney
Sydney, Australia
lu.qin@uts.edu.au

Wenjie Zhang
University of New South Wales
Sydney, Australia
zhangw@cse.unsw.edu.au

Abstract

The advancement of graph-based malware analysis is critically limited by the absence of large-scale datasets that capture the inherent hierarchical structure of software. Existing methods often oversimplify programs into single level graphs, failing to model the crucial semantic relationship between high-level functional interactions and low-level instruction logic. To bridge this gap, we introduce HiGRAPH, the largest public hierarchical graph dataset for malware analysis, comprising over **200M** Control Flow Graphs (CFGs) nested within **595K** Function Call Graphs (FCGs). This two-level representation preserves structural semantics essential for building robust detectors resilient to code obfuscation and malware evolution. We demonstrate HiGRAPH's utility through a large-scale analysis that reveals distinct structural properties of benign and malicious software, establishing it as a foundational benchmark for the community. The dataset and tools are publicly available at <https://higraph.org>.

CCS Concepts

• Security and privacy → Software security; • Computing methodologies → Neural networks.

Keywords

Android malware, Hierarchical Graph, Graph Neural Network, Malware Analysis

ACM Reference Format:

Han Chen, Hanchen Wang, Hongmei Chen, Ying Zhang, Lu Qin, and Wenjie Zhang. 2024. HiGRAPH: A Large-Scale Hierarchical Graph Dataset for Malware Analysis. In *Proceedings of the 30th ACM SIGKDD Conference on Knowledge Discovery and Data Mining (KDD '24)*, August 25–29, 2024, Barcelona, Spain. ACM, New York, NY, USA, 11 pages. <https://doi.org/XXXXXXX.XXXXXX>.

Permission to make digital or hard copies of all or part of this work for personal or classroom use is granted without fee provided that copies are not made or distributed for profit or commercial advantage and that copies bear this notice and the full citation on the first page. Copyrights for components of this work owned by others than the author(s) must be honored. Abstracting with credit is permitted. To copy otherwise, or republish, to post on servers or to redistribute to lists, requires prior specific permission and/or a fee. Request permissions from permissions@acm.org.
KDD '24, Barcelona, Spain

© 2024 Copyright held by the owner/author(s). Publication rights licensed to ACM.
ACM ISBN 978-1-4503-XXXX-X/24/08
<https://doi.org/XXXXXXX.XXXXXX>

```

1 // gain execution
2 FileList files = scanDirectory("C:/Users/User/Documents");
3
4 // encrypt files with a simple, hardcoded key
5 String key = "12345678";
6 for (file in files) {
7   encryptFile_XOR(file, key);
8 }
9
10 // send completion signal to C2 server
11 http.post(C2_SERVER_URL, "status=done");
12
13 // create ransom note
14 createRansomNote.TXT("Desktop/ransom.txt");
15 ...

```

```

1 // gain execution and set advanced persistence
2 setPersistence_ScheduledTask();
3
4 // scan local and network drives
5 FileList files = scanAllLocalDrives();
6 files.add(scanNetworkShares());
7
8 // communicate securely with C2 server
9 String rsa_pub_key = https.get(dga.getDomain() +
  "getMasterKey");
10
11 // prevent recovery and use hybrid encryption
12 deleteShadowCopies();
13 for (file in files) {
14   String session_key = generateAESKey();
15   encryptFile_AES(file, session_key);
16   String encrypted_session_key = encryptKey_RSA(session_key,
    rsa_pub_key);
17   appendKeyToFile(file, encrypted_session_key);
18 }
19
20 // show sophisticated ransom note
21 showRansomGUI();
22 ...

```

Figure 1: Motivating example: Evolution of CryptoLocker ransomware from V1 to V2. Despite significant changes in implementation details, both versions share a common behavioral skeleton: file discovery → encryption → notification. The core structural patterns remain detectable through graph-based analysis, demonstrating the necessity of modeling binaries as hierarchical graphs to capture persistent malicious behaviors across code evolution.

1 Introduction

Graph neural networks (GNNs) [12, 14, 25, 31] offer a promising frontier for malware analysis, as they can capture complex structural patterns resilient to common obfuscation techniques. However, the development of robust GNN-based detectors is severely hampered by the lack of large-scale, high-quality datasets. Existing malware corpora often suffer from critical limitations: they may not represent programs as graphs, or they possess temporal biases (e.g., training on "future" samples) that lead to unrealistic performance evaluations [3, 20]. More fundamentally, even public graph-based datasets like Malnet [16] typically represent programs as single-level, "flat" graphs. This oversimplification fails to capture the rich, hierarchical nature of software, where low-level control flow within functions and high-level interactions between them are both crucial for understanding program behavior.

The necessity of a hierarchical perspective is exemplified by the evolution of ransomware like CryptoLocker (Figure 1). While its implementation details changed significantly, evolving from simple XOR to hybrid AES+RSA encryption, its core malicious behavior remained a consistent three-stage skeleton: *file discovery* → *encryption* → *notification*. A traditional, flat graph representation

might miss this underlying structural similarity amidst the code changes. In contrast, a hierarchical representation, which models both the internal logic of functions (as Control Flow Graphs, CFGs) and the calls between them (as a Function Call Graph, FCG, see Figure 2), can identify this persistent malicious blueprint, enabling detection that transcends superficial code modifications.

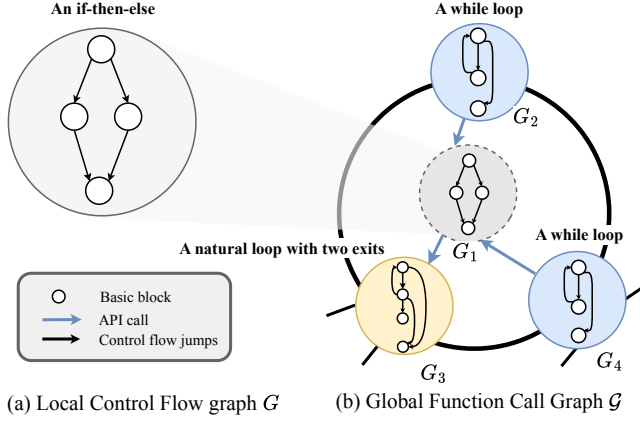


Figure 2: Illustration of key application analysis concepts: (a) Control Flow Graph G showing instruction sequences within functions, (b) Function Call Graph G depicting inter-function relationships (G_1 to G_4) via API calls. (1) to (3) shows typical control flow structures.

To address these challenges and enable more sophisticated analysis of program hierarchies, we introduce HiGRAPH, the largest publicly available hierarchical graph dataset for malware analysis. HiGRAPH encompasses 595,211 applications, represented as 595,211 global FCGs that contain a total of 201,792,085 local CFGs. This two-level structure explicitly captures both inter-procedural dependencies and intra-procedural logic. By providing granular hierarchical data with spatio-temporal consistency, HiGRAPH provides a robust foundation for building and evaluating the next generation of malware detectors. To facilitate exploration, we also provide an interactive website for the dataset at <https://higraph.org>.

In summary, our contributions are as follows:

- We introduce and release HiGRAPH, the largest hierarchical graph dataset for malware analysis. Its scale and explicit two-level structure are designed to overcome the limitations of existing flat-graph and non-graph corpora.
- We conduct a large-scale analysis on HiGRAPH, revealing key statistical properties and temporal trends in the structural complexity of benign and malicious software. This analysis demonstrates the unique insights enabled by a hierarchical perspective.
- We open-source HiGRAPH and our processing tools to provide a critical community resource. We aim to standardize the evaluation of hierarchical malware analysis methods and foster reproducible, high-impact research in AI for cybersecurity.

2 Related Work

Malware Datasets. Research in malware analysis is supported by numerous datasets. Large scale repositories like AndroZoo [1] for

Android and VirusShare [27] for Windows provide vast collections of raw malware samples. Other datasets offer more structured information, such as API call graphs from APIGraph [32] or network traffic from CICMalDroid [19]. However, among datasets designed for graph based analysis, MalNet [9] is the most prominent. While extensive, MalNet represents programs as flat graphs, overlooking the inherent hierarchical structure of software. This structural simplification limits the potential for more nuanced analysis, creating a need for datasets that capture the multilevel organization of program code.

Graph Representation Learning. Graph representation learning has rapidly evolved from early node embedding methods [11, 21] to a variety of powerful Graph Neural Networks (GNNs), such as Graph Convolutional Networks (GCNs) [15], Graph Attention Networks (GATs) [26], and transformer based architectures [22, 23]. These models have demonstrated strong performance in malware classification [6, 13]. Nevertheless, their effectiveness is primarily on conventional, non-hierarchical graphs, making them unable to directly leverage the nested relationships present in complex systems like software.

Hierarchical Graph Learning. To model systems with nested structures, the concept of hierarchical graphs, or Graphs of Graphs (GoG), has emerged [5, 17, 28]. This paradigm has been applied in fields such as computational biology [10, 29] and for detecting malware on Windows [18]. However, its application to Android malware has been unexplored, largely due to the absence of suitable datasets with explicit hierarchical information. To bridge this gap, we introduce HiGRAPH, a new, large scale dataset designed specifically for hierarchical graph learning on Android applications. As detailed in Table 1, HiGRAPH provides the first opportunity for the community to explore hierarchical representation learning for malware analysis at scale.

3 Dataset Construction

Our methodology for constructing the HiGRAPH dataset is illustrated in Figure 3. The process involves two primary stages: (1) collecting and curating a large-scale, longitudinal dataset of Android applications, and (2) extracting hierarchical graph representations (FCGs and CFGs) from each application.

3.1 Data Collection and Curation

We collected 595,211 Android applications from AndroZoo [2], a repository of apps spanning from 2012 to December 2022. We established ground truth labels by analyzing VirusTotal reports, obtained via their academic API. An application is labeled as malicious if detected by at least 15 antivirus engines, a common threshold in malware research. Benign samples are those with no detections. This process resulted in 57,184 malicious and 538,027 benign applications. For malware samples, we further use AVClass2 [24] to assign a fine-grained family label. Detailed statistics are presented in Table 2.

The dataset construction prioritizes two critical properties. First, **temporal consistency** is maintained by ensuring samples are distributed evenly across the 10-year collection period. This mitigates concept drift, where malware characteristics evolve over time. We

	Dataset Properties		Graph Features		Quality Assurance	
	Year	Size	Format	Scale	Temp.	Spat.
AndroZoo[1]	2016	11M+	Raw APKs	●	●	○
Drebin[4]	2014	5.5K	Features	○	●	○
AMD[30]	2017	NA ¹	Features	○	○	○
APIGraph[32]	2020	322K	Features	●	●	●
Malnet[16]	2021	1.2M	Single-level	●	○	○
HiGRAPH (Ours)	2025	595K	Hierarchical	●	●	●

^a ●=high/full, ○=low/none, ●=medium/partial.

^b Scale indicates data scale size. Temp.=Temporal bias robustness, Spat.=Spatial bias robustness. Format refers to the data representation used by each dataset.

¹ The dataset is no longer publicly available according to the authors.

Table 1: Comparison with existing malware datasets in terms of dataset properties, graph features, and quality assurance.

Table 2: Key statistics of our graph dataset, comparing malicious and benign applications.

Property	Malicious	Benign
Number of FCGs	57,184	538,027
Number of CFGs	6,925,406	194,866,679
<i>Average per FCG</i>		
Nodes	266.48	791.54
Edges	491.67	1414.51
<i>Average per CFG</i>		
Nodes	12.29	12.17
Edges	14.94	13.94

Table 3: Detailed graph statistics for the most prevalent malware families (subset of total 57,184 malicious samples), with benign applications included for a comparative baseline. All node and edge counts are per-graph averages.

Family	Benign	Adware	Tool	Downloader
Function Call Graph (FCG)				
# Apps (FCGs)	538,027	25,633	377	159
Avg. nodes	791.54	337.38	300.79	1,453.33
Avg. edges	1,414.51	615.80	531.73	3,370.85
Control Flow Graph (CFG)				
# Total CFGs	194,866,679	3,838,620	50,863	131,311
Avg. nodes	12.17	12.25	11.49	12.14
Avg. edges	13.94	14.94	13.83	14.56

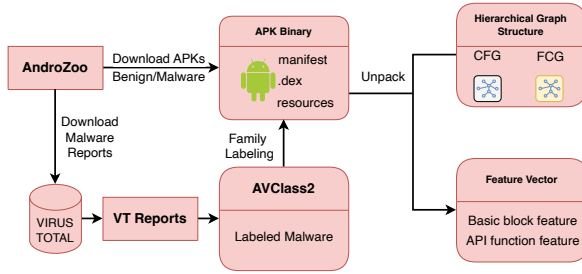


Figure 3: Overview of the HiGRAPH construction pipeline. We collect Android applications from AndroZoo, obtain VirusTotal reports for labeling, use AVClass2 for malware family classification, and extract hierarchical graph structures (CFGs and FCGs) with associated feature vectors.

limited our collection to applications up to December 2022 because research indicates antivirus detection results stabilize after approximately one year, ensuring more reliable ground truth labels. Second, **spatial consistency** is achieved by maintaining a realistic malware to benign ratio of approximately 1:9, mirroring real world distributions. This careful curation addresses common dataset biases that can lead to over-optimistic and unrealistic performance evaluations.

3.2 Hierarchical Graph Extraction

After curating the dataset, we use Androguard [7] to decompile each application and extract its program structure as a hierarchical graph. This representation consists of a single global Function Call Graph (FCG) per application, with each node in the FCG corresponding to a local function represented by its own Control Flow Graph (CFG). The final HiGRAPH contains over 200 million CFGs and nearly 600,000 FCGs, with detailed statistics in Table 3.

Function Call Graph (FCG). The FCG provides an inter-procedural view of an application. We model it as a directed graph $\mathcal{G} = (\mathcal{V}, \mathcal{E})$, where nodes \mathcal{V} are functions and edges \mathcal{E} represent calls between them. We distinguish between external functions provided by standard libraries and local functions custom-coded by developers. As malicious logic typically resides in local functions, our analysis focuses on the subgraph induced by these \mathcal{V}_{loc} . Furthermore, to reduce noise and focus on security relevant interactions, we apply high-sensitivity filters to retain only call graph edges that connect to sensitive APIs known to be associated with malicious activities.

Control Flow Graph (CFG). The CFG provides an intra-procedural view of a function’s logic. For each local function f , we construct its CFG, $G_f = (V_f, E_f)$, where each node $u \in V_f$ is a basic block (a sequence of non-branching instructions), and edges represent control flow transfers. To capture the semantics of each basic block, we engineer an 11-dimensional feature vector for each node, drawing

inspiration from prior work [18]. This vector summarizes the block from three perspectives: (1) **Instruction Semantics**, by counting seven categories of bytecode operations (e.g., arithmetic, logic, call); (2) **Content Metrics**, such as the total instruction count and the presence of constants; and (3) **Structural Properties**, represented by the block’s out-degree. Because these features are derived from bytecode, our representation is independent of the original source language (e.g., Java or Kotlin), making it robust to language evolution.

3.3 Dataset Reproducibility and Accessibility

Reproducibility. To foster reproducibility, we release our entire data processing pipeline as open-source software on GitHub. The repository includes all scripts for decompilation, graph extraction, and feature engineering, accompanied by comprehensive documentation. This allows other researchers to replicate our methodology precisely, extend it for new purposes, and ensure consistent data processing standards across studies.

Accessibility and Maintenance. The HiGRAPH and our processing tools are publicly available at <https://higraph.org> under a CC BY-NC-SA 4.0 license. Beyond direct downloads, the project website features an interactive interface for exploring the dataset, including tools for visualizing graph structures and statistical summaries. To ensure long-term value to the community, we have implemented a version control system and established a maintenance plan. This includes clear documentation of all updates and a community feedback mechanism to maintain data integrity.

4 Empirical Analysis

This section presents an empirical analysis of our dataset, focusing on the structural properties of Control Flow Graphs (CFGs) and Function Call Graphs (FCGs). We compare the characteristics of malicious and benign applications to uncover patterns that can inform the design and interpretation of graph based detection models.

4.1 Dataset-wide Statistical Overview

Table 1 compares HiGRAPH with other large scale hierarchical graph datasets. HiGRAPH offers significant contributions to cybersecurity research, primarily through its scale and complexity. With over 201M local CFGs and 595,211 global FCGs, it vastly exceeds prior datasets in size. The average number of nodes per local graph (741.10) highlights a higher structural complexity compared to domains like scientific publications (Arxiv, 30.9 nodes) or social networks (QQ, 291.2 nodes). While the average local edge count is lower (12.17), this reflects the inherent sparsity of software control flow structures. The scale and unique characteristics of HiGRAPH introduce new challenges and opportunities for developing robust, scalable graph based malware analysis models.

4.2 Malware Classification and Family Analysis

To provide fine grained malware categorization, we employ AV-Class2 [24] to generate standardized malware family labels from VirusTotal detection names. This process leverages the comprehensive taxonomy of AVClass2 to assign structured labels categorized

as Family (FAM), Behavior (BEH), Class (CLASS), and File Properties (FILE). This systematic approach ensures robust labeling and enables detailed analysis of malware characteristics across different categories.

Table 5 presents the distribution of malware samples across the most prevalent classes in HiGRAPH. The analysis reveals distinct structural patterns: *Grayware* represents the largest category with 27,018 samples, typically exhibiting moderate complexity with an average of 141.76 nodes per FCG. In contrast, *Adware* samples, while fewer in number (25,633), display significantly higher structural complexity with an average of 337.38 nodes per FCG and correspondingly higher edge counts (615.80 edges). This structural divergence reflects the different operational requirements of these malware types. Adware often requires more complex interaction mechanisms for advertisement delivery and user engagement tracking.

Notably, *Downloader* malware exhibits the highest structural complexity, with an average of 1,453.33 nodes and 3,370.85 edges per FCG, despite having only 159 samples. This elevated complexity reflects the sophisticated coordination required for payload delivery, network communication, and evasion techniques. The detailed breakdown of structural properties across malware classes (complete statistics available in Appendix A) provides valuable insights for developing class specific detection strategies and understanding the operational characteristics of different malware families.

4.3 Structural Comparison of Malicious and Benign Graphs

Our analysis of structural metrics, depicted in Figure 4, reveals distinct patterns that differentiate malicious and benign applications.

On the Function Call Graph (FCG) level, malware exhibits higher average and maximum PageRank values (Figure 4b). This indicates that malicious applications feature more influential functions and a more centralized overall architecture, where certain functions act as critical hubs for control flow or obfuscation.

On the Control Flow Graph (CFG) level, malware samples show higher node degrees (Figure 4c) and elevated cyclomatic complexity (Figure 4d). These characteristics point to more intricate conditional logic within individual functions. The presence of exceptionally high maximum values for these metrics suggests that malicious code not only is more complex on average but also contains specific, highly convoluted functions designed for obfuscation or to implement sophisticated malicious behaviors.

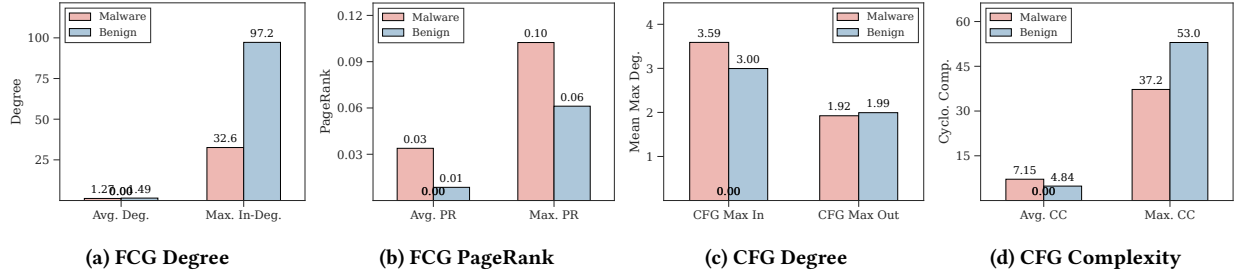
Collectively, these findings show that malicious software possesses more complex and centralized graph structures at both the inter-procedural (FCG) and intra-procedural (CFG) levels. The maximum values of these metrics, in particular, serve as strong indicators of malicious intent.

4.4 Temporal Evolution of Malware and Software Structure

Our comprehensive temporal analysis spanning the decade from 2012 to 2022 reveals distinct evolutionary patterns in malware families and fundamental structural changes in both malicious and benign software. This longitudinal perspective, enabled by HiGRAPH’s

Table 4: Comparison of HiGRAPH with other benchmark graph datasets. Our dataset is unique in its hierarchical structure and massive scale, especially in the number of individual graphs (local graphs).

Dataset	Field	Global Graph		Local Graph	
		# Global Graphs	Avg. Nodes	# Local Graphs	Avg. Nodes
CCI900 [5]	Chemical	1	25.4	14,343	25.4
CCI950 [5]	Chemical	1	26.2	7,606	26.2
NetBasedDDI [5]	Drug	1	24.8	596	24.8
ZhangDDI [5]	Drug	1	25.2	544	25.2
ChChMiner [5]	Drug	1	27.8	1,329	27.8
DeepDDI [5]	Drug	1	27.5	1,704	27.5
Arxiv [17]	Text	1	30.9	4,666	30.9
QQ [17]	Social	1	291.2	37,836	291.2
HiGRAPH	Cybersecurity	595,211	741.1	201,792,085	12.2

**Figure 4: Comparison of FCG and CFG structural metrics between malware and benign applications. Subfigures detail distributions for: (a) FCG In-Degree (Avg. vs. Max), (b) FCG PageRank (Avg. vs. Max), (c) CFG In/Out-Degree (Avg. vs. Max), and (d) CFG Cyclomatic Complexity (Avg. vs. Max).****Table 5: Malware class distribution and structural characteristics in HiGRAPH showing the top 7 most prevalent classes.**

Class	# FCGs	Avg. Nodes	Avg. Edges
Grayware	27,018	141.76	259.13
Adware	25,633	337.38	615.80
Tool	377	300.79	531.73
Downloader	159	1,453.33	3,370.85
Clicker	94	112.04	157.67
Spyware	46	439.07	793.15
Backdoor	45	238.44	411.71

temporal consistency, uncovers critical insights for understanding malware evolution and designing robust detection systems.

Malware Ecosystem Dynamics. The malware landscape exhibits clear dynamic behavior (Figure 5). The prevalence of top malware families fluctuates significantly, with families like *dowgin* and *sm-sreg* dominating specific periods (Figure 5a), illustrating the lifecycle of malware campaigns. Concurrently, the number of new, unique malware families grew exponentially until 2019 before declining (Figure 5b). This trajectory likely reflects the security arms race, mirroring the maturation of the Android platform and subsequent improvements in defense mechanisms.

Divergent Structural Evolution. A critical finding emerges when examining the temporal evolution of graph structural properties.

Benign applications demonstrate accelerating growth in both CFG and FCG complexity over time, particularly after 2016. Malware exhibits contrasting behavior: while CFG structures remain relatively stable and compact, FCG architectures show initial growth followed by shrinkage after 2015 and 2016. This suggests that malware has evolved toward smaller, more targeted functional units while maintaining sophisticated internal logic.

More significantly, density analysis reveals opposing trends between benign and malicious software. Benign applications become increasingly modular (lower density) despite size growth, characteristic of maintainable software engineering practices. Conversely, malware density increases over time, with FCG density showing particularly striking growth. This trend indicates that even as malware size decreases, constituent functions become more tightly interconnected. This likely reflects intentional architectural optimization for obfuscation and operational efficiency within constrained detection footprints.

Implications for Detection. These temporal patterns have profound implications for malware detection. The observed structural divergence suggests that density based metrics may serve as increasingly powerful discriminative features. The tendency of malware to maintain high structural density while benign software favors modularity provides a fundamental architectural signature that persists

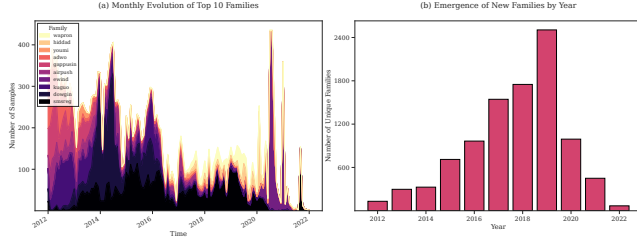


Figure 5: Temporal evolution of malware families in HiGRAPH. (a) Monthly distribution of top 10 malware families showing their prevalence over time, with distinct emergence and decline patterns. (b) Annual count of unique malware families, demonstrating the rapid emergence of new variants peaking around 2019-2020.

across temporal evolution. This finding underscores the value of HiGRAPH’s longitudinal design for understanding persistent malware characteristics amid evolving threat landscapes.

4.5 Correlation Analysis of Structural Metrics

To understand the interplay between centrality and complexity, we analyze the correlation between FCG PageRank and CFG cyclomatic complexity (Figures 6a and 6b). Malware and benign applications exhibit starkly different patterns.

Malware shows a moderate positive correlation ($R = 0.48$) between a function’s centrality (average PageRank) and its logical complexity (average cyclomatic complexity). This suggests a deliberate design where the most influential functions are also the most convoluted, likely to obfuscate core malicious logic. In contrast, benign software displays a weak negative correlation ($R = -0.18$). This fundamental structural divergence serves as a powerful signal for distinguishing between malicious and benign code.

4.6 Analysis of API Usage Patterns

An analysis of API call frequencies, visualized in Figure 7, provides a functional fingerprint of the applications in HiGRAPH. The usage patterns reveal a clear distinction between ubiquitous, general purpose APIs and platform specific APIs with high security relevance. The former category includes foundational APIs for file I/O (*java.io/File*), networking (*java.net/URLConnection*), and string manipulation, which are essential for standard application behavior. The latter category, however, features Android specific functions like *android.telephony/TelephonyManager*. While essential for some legitimate apps, their widespread presence is a strong indicator of potential risk, as these APIs are primary targets for exploitation by malware to steal sensitive information or perform unauthorized actions. This distinction in API usage provides a powerful, high level signal that can be leveraged for feature engineering to improve malware detection models.

5 Evaluating HiGRAPH for Malware Analysis

We evaluate HiGRAPH on core malware analysis tasks to demonstrate its effectiveness. Our central hypothesis is that HiGRAPH’s hierarchical structure, which combines intraprocedural Control Flow Graphs (CFGs) with an interprocedural Function Call Graph

(FCG), captures rich program semantics. This structure, we argue, leads to more robust and accurate malware detection. Specifically, we seek to answer the following research questions:

- **RQ1:** How do graph representation learning methods perform on HiGRAPH for malware detection?
- **RQ2:** How effectively does the hierarchical graph structure capture program semantics?
- **RQ3:** How does the hierarchical information in HiGRAPH enhance malware detection and classification accuracy?
- **RQ4:** What advantages does HiGRAPH’s hierarchical representation offer over traditional, single-level graph approaches?

5.1 Malware Detection and Classification (RQ1 & RQ3)

We first evaluate HiGRAPH on malware detection. We formulate two tasks: (1) a binary classification task to distinguish benign from malicious software, and (2) a multiclass classification task to categorize malware into families. For the latter, we use the five most frequent malware families in HiGRAPH due to class imbalance.

Models. We evaluate several graph neural networks (GNNs). As baselines that operate only on the function call graph (FCG), we use Graph Convolutional Networks (GCN) [14], Graph Attention Networks (GAT) [25], Graph Isomorphism Networks (GIN) [31], and GraphSAGE [12]. All baseline models employ a consistent architecture comprising two GNN layers with ReLU activation, followed by global mean pooling and a fully connected classification layer with logarithmic softmax output.

We also propose Hi-GNN, a hierarchical graph neural network designed to process both local Control Flow Graphs (CFGs) and the global Function Call Graph (FCG). Hi-GNN employs distinct GNN encoders for CFGs and FCGs, each utilizing the same two-layer architecture as the baselines. The learned multi-level representations are subsequently integrated through a fusion mechanism and passed to a final classification layer. This design enables Hi-GNN to capture both intra-procedural control flow patterns and inter-procedural functional dependencies simultaneously.

Experimental Setup. We split HiGRAPH into training, validation, and test sets with a 70/15/15 ratio, ensuring temporal consistency across splits. For CFGs, we extract an 11-dimensional feature vector for each node from its basic block’s assembly instructions, including counts of call, transfer, arithmetic, logic, compare, move, and termination instructions, as well as data declarations, total instructions, string/integer constants, and the number of successor blocks. For FCGs, node features consist of in-degree, out-degree, and total degree to ensure a fair comparison across models.

All models are trained using the Adam optimizer with learning rates selected from 0.0001, 0.001, 0.01 and batch sizes from 32, 64, 128. Hidden dimensions are tested across 64, 128, 256, with dropout rates of 0.4, 0.5, 0.6 applied to prevent overfitting. Training is conducted for up to 200 epochs with early stopping based on validation performance. We use PR-AUC, Macro F1, Precision, and Recall as evaluation metrics, focusing on Macro F1 due to the inherent class imbalance (approximately 10% malware samples). Each experiment is repeated three times with different random seeds, and we report the mean and standard deviation to ensure statistical reliability.

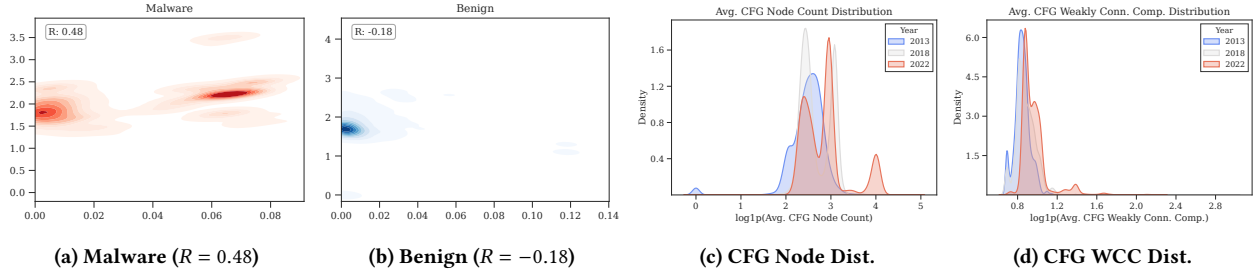


Figure 6: Correlation and temporal trend analysis. (a-b) 2D density plots of FCG Avg. PageRank vs. Avg. CFG Cyclomatic Complexity for Malware and Benign applications. (c-d) Yearly distributions of Avg. CFG Node Count and Avg. CFG WCC Count.



Figure 7: Word cloud of frequent API function names in HiGRAPH, where font size reflects usage frequency. The visualization highlights both common utility APIs (e.g., file I/O, networking) and security sensitive platform APIs (e.g., TelephonyManager).

Results. The malware detection results are in Table 6. All evaluated GNNs achieve reasonable Macro F1 scores, confirming their suitability for learning malware patterns from HiGRAPH. Our hierarchical model, Hi-GNN, significantly outperforms the single-level GNNs, with its superior Macro F1 score demonstrating that leveraging HiGRAPH’s multilevel structure yields more comprehensive program representations and improved detection accuracy.

Performance Analysis Across Malware Classes. Analysis of per-class performance reveals varying detection difficulty across malware types. *Grayware* and *Adware*, being the most prevalent classes with substantial training samples, achieve the highest detection accuracy across all models. However, smaller classes like *Backdoor* and *Spyware* present greater challenges due to limited representation in the training set. Notably, Hi-GNN demonstrates more consistent performance across all classes, suggesting that hierarchical representations provide more robust feature learning even for underrepresented malware families. The model shows particular strength in detecting structurally complex malware types like *Downloader*, where the intricate inter-procedural relationships captured by the FCG level prove most beneficial.

5.2 Temporal Robustness to Malware Evolution (RQ2 & RQ4)

Malware constantly evolves, causing a phenomenon known as "concept drift" where detection models quickly become outdated, a problem often called "model aging" [32]. To evaluate the ability of models to resist this degradation (their temporal robustness), we

Table 6: Malware detection performance. Results show mean \pm standard deviation for PR-AUC and Macro F1 scores. Best performance in each column is in bold.

Model	Binary Classification		Multi-class Classification	
	PR-AUC	Macro F1	PR-AUC	Macro F1
GCN	0.627 \pm 0.025	0.640 \pm 0.022	0.492 \pm 0.018	0.383 \pm 0.025
GAT	0.641 \pm 0.012	0.719 \pm 0.021	0.514 \pm 0.015	0.412 \pm 0.021
GIN	0.615 \pm 0.035	0.690 \pm 0.021	0.508 \pm 0.022	0.401 \pm 0.024
GraphSAGE	0.619 \pm 0.014	0.678 \pm 0.017	0.501 \pm 0.019	0.392 \pm 0.023
Hi-GNN	0.636 \pm 0.011	0.734 \pm 0.010	0.528 \pm 0.014	0.435 \pm 0.019

conduct an experiment using a temporal data split. We train models on data from 2012 and test their performance monthly on data from 2013 to assess short-term robustness. We also extend the test period to December 2016 to evaluate long-term robustness against more significant drift.

We quantify performance sustainability using the Area Under Time (AUT) for the Macro F1 score, or AUT(F1) [32]. AUT aggregates a model’s performance over a time period, calculated with Equation 1, where f is the Macro F1 score and N is the number of months. Higher AUT values (from 0 to 1) indicate greater robustness to concept drift.

$$AUT(f, N) = \frac{1}{N-1} \sum_{k=0}^{N-1} \frac{[f(k+1) + f(k)]}{2} \quad (1)$$

The results are shown in Table 7. Our hierarchical model, Hi-GNN, demonstrates superior temporal robustness in both scenarios. For the 2012–2013 split, Hi-GNN achieves an AUT(F1) of 0.755, outperforming all single-level GNNs (which score between 0.604–0.743). This advantage persists over the longer 2012–2016 period, where Hi-GNN scores 0.715, again surpassing the baselines.

This sustained performance answers RQ2 and RQ4, showing that the hierarchical structure of HiGRAPH is key to mitigating model aging. Hi-GNN leverages this structure to learn more fundamental malware characteristics. Specifically, it captures two levels of semantics: (1) The fine-grained CFGs represent core programming logic (e.g., loops, API calls) that remains relatively stable even as malware evolves, providing semantic invariance. (2) The global FCG captures the overall program architecture, which allows the model to adapt to structural changes in malware families over time.

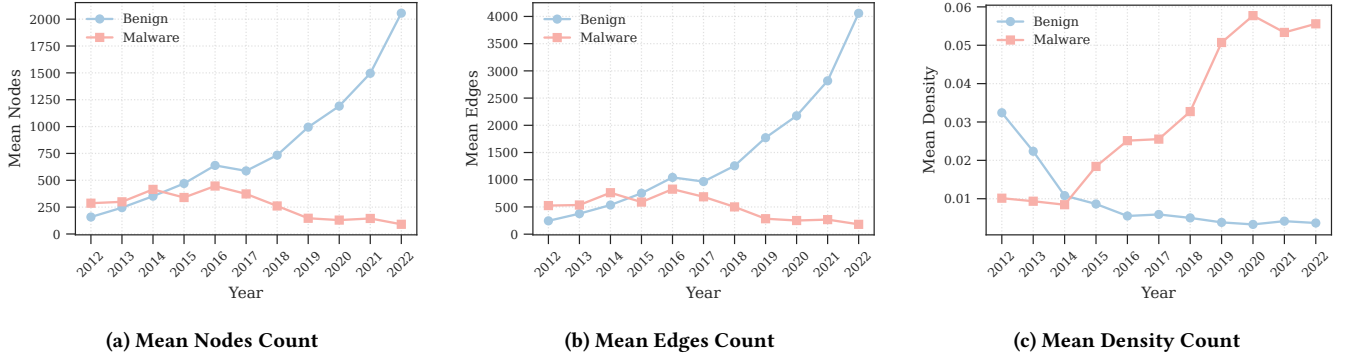


Figure 8: Trends in Function Call Graph (FCG) structural properties over time, showing mean nodes, mean edges, and mean density.

Table 7: Malware evolution detection. Models are trained on 2012 data and tested on future years. Results are AUT (Area Under Time-series) for PR-AUC and Macro F1 scores, shown as mean \pm std. dev.

Model	2012 \rightarrow 2013		2012 \rightarrow 2016	
	PR-AUC	Macro F1	PR-AUC	Macro F1
GCN	0.516 \pm 0.015	0.604 \pm 0.021	0.489 \pm 0.018	0.572 \pm 0.024
GAT	0.513 \pm 0.012	0.691 \pm 0.018	0.483 \pm 0.014	0.651 \pm 0.020
GIN	0.550 \pm 0.019	0.743 \pm 0.023	0.520 \pm 0.021	0.703 \pm 0.025
GraphSAGE	0.518 \pm 0.014	0.612 \pm 0.019	0.489 \pm 0.016	0.574 \pm 0.021
Hi-GNN	0.564 \pm 0.011	0.755 \pm 0.017	0.498 \pm 0.026	0.715 \pm 0.019

By integrating these two views, Hi-GNN can identify persistent behavioral patterns that transcend temporal shifts.

5.3 Temporal Evolution of Graph Structures

To better understand the structural evolution of malware and benign software, we analyze temporal trends in their Function Call Graph (FCG) properties (Figure 8). This analysis reveals divergent evolutionary patterns that underscore the challenges of long-term malware detection. A corresponding analysis of Control Flow Graph (CFG) evolution is in Appendix B.

Our analysis reveals two key trends. First, examining graph size (Figure 8a-b), benign FCGs show accelerating growth, indicating increasing software complexity. In contrast, malware FCGs tend to shrink after 2015, suggesting a shift toward smaller, more targeted functional units.

Second, analyzing graph density (Figure 8c), benign FCGs become sparser, which is characteristic of modular design. Conversely, malware FCG density substantially increases, indicating that even as overall size decreases, functions become more tightly interconnected. This may reflect sophisticated obfuscation or a concentration of capabilities in a densely linked core.

These findings demonstrate that benign and malicious applications exhibit divergent evolutionary patterns. Benign applications evolve toward sustainable growth and modularity. In contrast, malware architecture appears optimized for functional concentration

and a reduced footprint. These insights underscore the different development paradigms and highlight the structural dynamics that detection models must navigate.

6 Conclusion

We introduced HiGRAPH, a large-scale, hierarchical graph dataset for malware analysis that integrates millions of fine-grained Control Flow Graphs within a global Function Call Graph. We demonstrated that this structure, capturing both intraprocedural and interprocedural program semantics, provides a richer foundation for analysis than traditional flat graph representations.

Our experiments showed that a hierarchical model, Hi-GNN, significantly outperforms single-level GNNs in malware detection. Crucially, Hi-GNN also exhibits strong temporal robustness, mitigating the "model aging" effect by learning persistent patterns from both local and global graph structures as malware evolves. The hierarchical representation proves particularly effective for concept drift adaptation, enabling robust detection of both pre-drift and post-drift malware samples through its dual-level semantic invariance and structural adaptation capabilities.

This finding underscores the value of hierarchical representations for building resilient security systems capable of adapting to evolving threat landscapes. By providing stable semantic features at the CFG level and adaptive architectural patterns at the FCG level, HiGRAPH enables more effective cross-temporal generalization than traditional single-level approaches.

We have publicly released HiGRAPH to foster new research in robust malware analysis and concept drift adaptation. We believe this work is a key step toward building next-generation defense systems capable of combating sophisticated and evolving cyber threats through hierarchical graph contrastive learning approaches.

References

- [1] Kevin Allix, Tegawendé F. Bissyandé, Jacques Klein, and Yves Le Traon. 2016. Androzoo: Collecting millions of android apps for the research community. In *Proceedings of the 13th international conference on mining software repositories*. 468–471.
- [2] Kevin Allix, Tegawendé F. Bissyandé, Jacques Klein, and Yves Le Traon. 2016. AndroZoo: Collecting Millions of Android Apps for the Research Community. In *Proceedings of the 13th International Conference on Mining Software Repositories (Austin, Texas) (MSR '16)*. ACM, New York, NY, USA, 468–471. doi:10.1145/2901739.2903508

- [3] Daniel Arp, Erwin Quiring, Feargus Pendlebury, Alexander Warnecke, Fabio Pierazzi, Christian Wressnegger, Lorenzo Cavallaro, and Konrad Rieck. 2022. Dos and don'ts of machine learning in computer security. In *31st USENIX Security Symposium (USENIX Security 22)*. 3971–3988.
- [4] Daniel Arp, Michael Spreitzenbarth, Malte Hubner, Hugo Gascon, Konrad Rieck, and CERT Siemens. 2014. Drebin: Effective and explainable detection of android malware in your pocket.. In *Ndss*, Vol. 14. 23–26.
- [5] Han Chen, Hanchen Wang, Hongmei Chen, Ying Zhang, Wenjie Zhang, and Xuemin Lin. 2023. Denoising variational graph of graphs auto-encoder for predicting structured entity interactions. *IEEE Transactions on Knowledge and Data Engineering* 36, 3 (2023), 1016–1029.
- [6] Yi-Hsien Chen, Si-Chen Lin, Szu-Chun Huang, Chin-Laung Lei, and Chun-Ying Huang. 2023. Guided malware sample analysis based on graph neural networks. *IEEE Transactions on Information Forensics and Security* 18 (2023), 4128–4143.
- [7] Anthony Desnos and Geoffrey Gueguen. 2018. Androguard documentation. *Obtenido de Androguard* (2018).
- [8] Matthias Fey and Jan E. Lenssen. 2019. Fast Graph Representation Learning with PyTorch Geometric. In *ICLR Workshop on Representation Learning on Graphs and Manifolds*.
- [9] Scott Freitas, Yuxiao Dong, Joshua Neil, and Duen Horng Chau. 2020. A large-scale database for graph representation learning. *arXiv preprint arXiv:2011.07682* (2020).
- [10] Ziqi Gao, Chenran Jiang, Jiawen Zhang, Xiaosen Jiang, Lanqing Li, Peilin Zhao, Huanming Yang, Yong Huang, and Jia Li. 2023. Hierarchical graph learning for protein-protein interaction. *Nature Communications* 14, 1 (2023), 1093.
- [11] Aditya Grover and Jure Leskovec. 2016. node2vec: Scalable feature learning for networks. In *Proceedings of the 22nd ACM SIGKDD international conference on Knowledge discovery and data mining*. 855–864.
- [12] Will Hamilton, Zitao Ying, and Jure Leskovec. 2017. Inductive representation learning on large graphs. *Advances in neural information processing systems* 30 (2017).
- [13] Yiling He, Yiping Liu, Lei Wu, Ziqi Yang, Kui Ren, and Zhan Qin. 2022. Msroid: Identifying malicious snippets for android malware detection. *IEEE Transactions on Dependable and Secure Computing* 20, 3 (2022), 2025–2039.
- [14] Thomas N Kipf and Max Welling. 2016. Semi-supervised classification with graph convolutional networks. *arXiv preprint arXiv:1609.02907* (2016).
- [15] Thomas N Kipf and Max Welling. 2017. Semi-supervised classification with graph convolutional networks. *arXiv preprint arXiv:1609.02907* (2017).
- [16] Ce Li, Zijun Cheng, He Zhu, Leiqi Wang, Qiujuan Lv, Yan Wang, Ning Li, and Degang Sun. 2022. DMalNet: Dynamic malware analysis based on API feature engineering and graph learning. *Computers & Security* 122 (2022), 102872.
- [17] Jia Li, Yu Rong, Hong Cheng, Helen Meng, Wenbing Huang, and Junzhou Huang. 2019. Semi-supervised graph classification: A hierarchical graph perspective. In *The World Wide Web Conference*. 972–982.
- [18] Xiang Ling, Lingfei Wu, Wei Deng, Zhenqing Qu, Jiangyu Zhang, Sheng Zhang, Tengfei Ma, Bin Wang, Chunming Wu, and Shouling Ji. 2022. MalGraph: Hierarchical graph neural networks for robust windows malware detection. In *IEEE INFOCOM 2022-IEEE Conference on Computer Communications*. IEEE, 1998–2007.
- [19] Samaneh MahdaviFar, Andi Fitriah Abdul Kadir, Rasool Fatemi, Dima Alhadidi, and Ali A Ghorbani. 2020. Dynamic android malware category classification using semi-supervised deep learning. In *2020 IEEE Intl Conf on Dependable, Autonomic and Secure Computing, Intl Conf on Pervasive Intelligence and Computing, Intl Conf on Cloud and Big Data Computing, Intl Conf on Cyber Science and Technology Congress (DASC/PiCom/CyberSciTech)*. IEEE, 515–522.
- [20] Feargus Pendlebury, Fabio Pierazzi, Roberto Jordaney, Johannes Kinder, and Lorenzo Cavallaro. 2019. {TESSERACT}: Eliminating experimental bias in malware classification across space and time. In *28th USENIX security symposium (USENIX Security 19)*. 729–746.
- [21] Bryan Perozzi, Rami Al-Rfou, and Steven Skiena. 2014. DeepWalk: Online learning of social representations. In *Proceedings of the 20th ACM SIGKDD international conference on Knowledge discovery and data mining*. 701–710.
- [22] Ladislav Rampásek, Michael Galkin, Vijay Prakash Dwivedi, Anh Tuan Luu, Guy Wolf, and Dominique Beaini. 2022. Recipe for a general, powerful, scalable graph transformer. *Advances in Neural Information Processing Systems* 35 (2022), 14501–14515.
- [23] Yu Rong, Yatao Bian, Tingyang Xu, Weiyang Xie, Ying Wei, Wenbing Huang, and Junzhou Huang. 2020. Self-supervised graph transformer on large-scale molecular data. *Advances in neural information processing systems* 33 (2020), 12559–12571.
- [24] Silvia Sebastián and Juan Caballero. 2020. Avclass2: Massive malware tag extraction from av labels. In *Proceedings of the 36th Annual Computer Security Applications Conference*. 42–53.
- [25] Petar Veličković, Guillem Cucurull, Arantxa Casanova, Adriana Romero, Pietro Lio, and Yoshua Bengio. 2017. Graph attention networks. *arXiv preprint arXiv:1710.10903* (2017).
- [26] Petar Veličković, Guillem Cucurull, Arantxa Casanova, Adriana Romero, Pietro Lio, and Yoshua Bengio. 2018. Graph attention networks. *arXiv preprint arXiv:1710.10903* (2018).
- [27] VirusShare. 2025. VirusShare.com. <https://virusshare.com/>. [Accessed on 05/14/2025].
- [28] Hanchen Wang, Defu Lian, Ying Zhang, Lu Qin, and Xuemin Lin. 2020. Gognn: Graph of graphs neural network for predicting structured entity interactions. *arXiv preprint arXiv:2005.05537* (2020).
- [29] Yingheng Wang, Yaosen Min, Xin Chen, and Ji Wu. 2021. Multi-view graph contrastive representation learning for drug-drug interaction prediction. In *Proceedings of the web conference 2021*. 2921–2933.
- [30] Fengguo Wei, Yuping Li, Sankardas Roy, Xinming Ou, and Wu Zhou. 2017. Deep ground truth analysis of current android malware. In *Detection of Intrusions and Malware, and Vulnerability Assessment: 14th International Conference, DIMVA 2017, Bonn, Germany, July 6-7, 2017, Proceedings 14*. Springer, 252–276.
- [31] Keyulu Xu, Weihua Hu, Jure Leskovec, and Stefanie Jegelka. 2018. How powerful are graph neural networks? *arXiv preprint arXiv:1810.00826* (2018).
- [32] Jing Zhang, Zhao Feng Zhang, Dandan Wu, Yifei Li, Sen Zhang, Hai Jin, and Di Wu. 2020. Enhancing state-of-the-art classifiers with api semantics to detect evolved android malware. In *Proceedings of the 2020 ACM SIGSAC Conference on Computer and Communications Security*. 1883–1898.

A Extended Dataset Statistics

This appendix provides comprehensive statistical details that supplement the malware classification analysis presented in Section 4.2 of the main paper. The complete breakdowns presented here enable detailed analysis of structural patterns across all identified malware classes and support reproducible research.

B Extended Temporal Analysis

This section provides a detailed temporal analysis of Control Flow Graph (CFG) properties, supplementing the main paper's discussion on Function Call Graph (FCG) evolution.

Examining the temporal evolution of CFGs (Figure 9), we observe that benign applications show accelerating growth in both nodes and edges, particularly after 2016. This indicates increasing intra-procedural complexity. In contrast, malware CFGs remain small and relatively stable over time.

Analyzing graph density, benign CFGs become sparser over time despite their growth in size, suggesting a trend towards more structured and less complex functions. Conversely, malware CFG density remains consistently higher than that of benign software after 2014. This points to more intricate internal logic within smaller functions, possibly as a result of obfuscation techniques.

C Complete Experimental Configuration

This section provides comprehensive experimental details that supplement the experimental setup described in Section 5 of the main paper. All technical specifications and hyperparameter configurations are documented here to ensure full reproducibility.

C.1 Detailed Model Architectures

The model architectures detailed in the main paper are expanded here with specific implementation details. For the baseline GNN models (GCN, GAT, GIN, GraphSAGE) used for graph-level classification, we employ a consistent architecture comprising two GNN layers with ReLU activation functions, followed by global mean pooling and a fully connected classification layer with logarithmic softmax output. Dropout regularization is applied uniformly across baseline models.

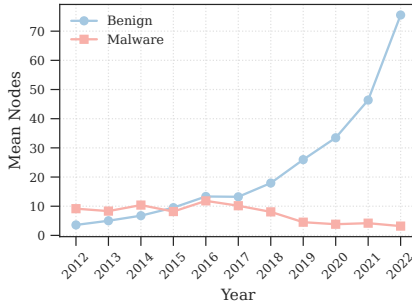
Hi-GNN employs a dual-encoder architecture with separate GNN encoders for CFGs and FCGs. Each encoder uses the same two-layer structure as the baselines, with learned representations integrated

Table 8: Detailed Function Call Graph (FCG) Statistics by Malware Class

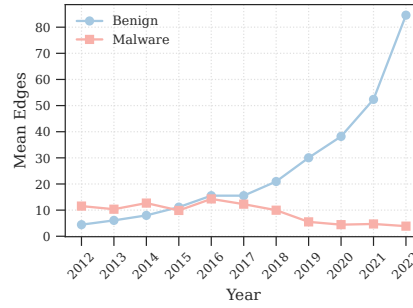
Class	# FCGs	Nodes			Edges			Average Degree			Density		
		Min	Mean	Max	Min	Mean	Max	Min	Mean	Max	Min	Mean	Max
Grayware	27,018	2	141.76	9,901	4	259.13	24,354	0	2.02	5.60	0.01	0.10	1.00
Adware	25,633	2	337.38	7,241	4	615.80	17,700	0	3.04	8.62	0.02	0.03	1.00
Tool	377	9	300.79	2,182	7	531.73	4,470	1.54	2.91	5.69	0.01	0.02	0.19
Downloader	159	3	1,453.33	12,326	2	3,370.85	31,292	1.17	3.01	5.26	0.02	0.04	0.67
Clicker	94	3	112.04	706	2	157.67	1,221	1.33	2.25	4.00	0.01	0.09	0.67
Spyware	46	32	439.07	2,320	35	793.15	4,837	2.00	2.85	4.67	0.01	0.03	0.07
Backdoor	45	19	238.44	1,626	18	411.71	3,302	1.84	2.65	4.22	0.01	0.03	0.11

Table 9: Detailed Control Flow Graph (CFG) Statistics by Malware Class

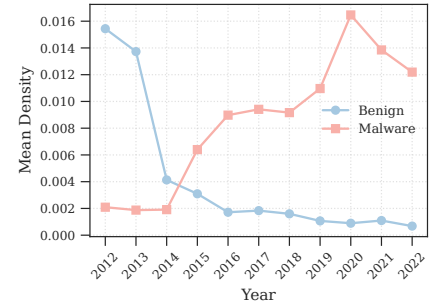
Class	# CFGs	Nodes			Edges			Average Degree			Density		
		Min	Mean	Max	Min	Mean	Max	Min	Mean	Max	Min	Mean	Max
Adware	3,838,620	2	12.25	1,281	1	14.94	2,238	0.20	2.20	8.50	0.02	0.39	2.83
Grayware	1,750,737	2	12.73	932	1	15.62	1,455	0.20	2.20	26.00	0.02	0.38	8.50
Downloader	131,311	2	12.14	2,093	1	14.56	2,117	0.33	2.18	4.80	0.01	0.39	2.33
Tool	50,863	2	11.49	591	1	13.83	742	0.29	2.16	5.77	0.01	0.39	2.00
Spyware	9,827	2	11.27	718	1	13.71	917	0.40	2.21	3.69	0.01	0.38	1.00
Backdoor	4,718	3	12.35	369	1	14.92	582	0.50	2.15	3.38	0.01	0.38	1.00
Clicker	3,741	2	12.18	199	1	14.26	249	0.50	2.10	4.51	0.01	0.38	1.00



(a) Mean Nodes Count



(b) Mean Edges Count



(c) Mean Density Count

Figure 9: Trends in Control Flow Graph (CFG) structural properties over time, showing mean nodes, mean edges, and mean density.

through concatenation followed by a linear transformation before the final classification layer.

C.2 Baseline Methods

We compare the performance of Hi-GNN against several widely-adopted GNN baseline models. These models are standard benchmarks for graph classification tasks:

- **Graph Convolutional Network (GCN)** [15]: Aggregates information from immediate neighbors using spectral graph convolutions.
- **Graph Attention Network (GAT)** [26]: Employs attention mechanisms to assign different weights to neighbor contributions during feature aggregation.
- **Graph Isomorphism Network (GIN)** [31]: A GNN variant designed to be as expressive as the Weisfeiler-Lehman graph isomorphism test, utilizing MLPs for node feature transformation and sum aggregation.

- **GraphSAGE** [12]: An inductive learning framework that samples a fixed number of neighbors and applies various aggregator functions (e.g., mean, LSTM, pooling) to combine neighbor features.
- **Hi-GNN**: A hierarchical graph neural network designed to process both local Control Flow Graphs (CFGs) and the global Function Call Graph (FCG). We use GCN as the GNN encoder for both CFG and FCG.

All baseline models were implemented using the PyTorch Geometric library [8].

C.3 Hyperparameters

We test on the hyperparameter settings shown in Table 10 and select the best configuration based on model performance. All models were trained using the Adam optimizer and cross-entropy loss function.

Table 10: Hyperparameter settings for GNN models. Hi-GNN contains separate encoders for CFG and FCG.

Model	Parameter	Value Range
Baseline GNNs	GNN Layers	1-3
	Hidden Dimension	64, 128, 256
	Batch Size	32, 64, 128
	Pooling Layer	Global Mean
	Learning Rate	0.001, 0.01
	Number of Epochs	50, 100, 200
Hi-GNN Encoder	Dropout Rate	0.4, 0.5, 0.6
	GNN Layers	1-3
	Hidden Dimension	64, 128, 256
	Batch Size	32, 64, 128, 256
	Pooling Layer	Global Mean
	Learning Rate	0.001, 0.01
	Number of Epochs	50, 100, 200
	Dropout Rate	0.4, 0.5, 0.6

D Computational Resources

Our data preprocessing pipeline, including downloading, preprocessing, decompilation, and label extraction, was performed on the Neptune cluster running RHEL 8.8. Each node in this cluster features dual AMD EPYC 9354 processors at 3.25GHz with 32 cores, 768GB of 4800MHz DDR5-RAM in twelve-channel configuration. We also have 20TB of project storage for storing the dataset.

The model training was conducted on the Saturn cluster, also running RHEL 8.8. The compute nodes are equipped with AMD EPYC 9254 processors running at 2.9GHz with 24 cores, 192GB of 4800MHz DDR5-RAM in twelve-channel configuration, dual 1.92TB NVMe SSD drives, and two NVIDIA L40 GPUs per node, each featuring 48GB of memory.

E Dataset Hosting

Our dataset and code are publicly available on GitHub, including preprocessing scripts and model implementations. An accompanying interactive website, higraph.org, provides tools for dataset exploration and graph structure visualization.

The website showcases curated sample graphs illustrating Control Flow Graph (CFG) and Function Call Graph (FCG) patterns of various malware families. The GitHub repository is actively maintained and includes detailed documentation to facilitate reproducible research. Both platforms are regularly updated to ensure reliable access and support the research community.

F License

The dataset and code are released under the Creative Commons Attribution-NonCommercial-ShareAlike 4.0 International License (CC BY-NC-SA 4.0). This license allows others to remix, adapt, and build upon our work non-commercially, as long as they credit us and license their new creations under identical terms.